LETTER • OPEN ACCESS

Isotope effects on intrinsic rotation in hydrogen, deuterium and tritium plasmas

To cite this article: M.F.F. Nave *et al* 2023 *Nucl. Fusion* **63** 044002

OPEN ACCESS
IOP Publishing | International Atomic Energy Agency

Nuclear Fusion

Nucl. Fusion 63 (2023) 044002 (6pp)

https://doi.org/10.1088/1741-4326/acbb8c

Letter

Isotope effects on intrinsic rotation in hydrogen, deuterium and tritium plasmas

M.F.F. Nave[1,*], **E. Delabie**[2], **J. Ferreira**[1], **J. Garcia**[5], **D. King**[6], **M. Lennholm**[6], **B. Lomanowski**[2], **F. Parra**[9], **P.R. Fernandez**[10], **J. Bernardo**[6], **M. Baruzzo**[4], **M. Barnes**[3], **F. Casson**[6], **J.C. Hillesheim**[6], **A. Hubber**[7], **E. Joffrin**[5], **A. Kappatou**[8], **C.F. Maggi**[6], **A. Mauriya**[1], **L. Meneses**[13], **M. Romanelli**[11], **F. Salzedas**[1,12] **and JET Contributors**[a]

EUROfusion Consortium, JET, Culham Science Centre, Abingdon OX14 3DB, United Kingdom of Great Britain and Northern Ireland
[1] Instituto de Plasmas e Fusão Nuclear, Instituto Superior Técnico, Universidade de Lisboa, Lisboa, P1049-001, Portugal
[2] Oak Ridge National Laboratory, Oak Ridge, TN 37831-6169, United States of America
[3] Rudolf Peierls Centre for Theoretical Physics, Oxford University, Oxford, United Kingdom of Great Britain and Northern Ireland
[4] ENEA C. R. Frascati, via E. Fermi 45, 00044 Frascati (Roma), Italy
[5] CEA, IRFM, F-13108 Saint Paul Lez Durance, France
[6] CCFE, Culham Centre for Fusion Energy, Culham Science Centre, Abingdon OX14 3DB, United Kingdom of Great Britain and Northern Ireland
[7] Institut für Energie- und Klimaforschung, Plasmaphysik, 52425 Jülich, Germany
[8] Max-Planck-Institut für Plasmaphysik, D-85748 Garching, Germany
[9] Princeton Plasma Physics Laboratory, Princeton, NJ 08540, United States of America
[10] MIT Plasma Science and Fusion Centre, Cambridge, MA 02139, United States of America
[11] Tokamak Energy Ltd, 173 Brook Drive, Milton Park, Oxfordshire OX14 4SD, United Kingdom of Great Britain and Northern Ireland
[12] Universidade do Porto, Faculdade de Engenharia, 4200-465 Porto, Portugal
[13] ITER Organization, Route de Vinon-sur-Verdon, CS 90 046, St. Paul Lez Durance, France

E-mail: mfn@ipfn.ist.utl.pt

Received 22 November 2022, revised 5 January 2023
Accepted for publication 13 February 2023
Published 9 March 2023

Abstract
The isotope effect on intrinsic rotation was studied at the Joint European Torus (JET) tokamak. With the unique capability of JET to operate with tritium (T), for the first time, experiments in hydrogen (H), deuterium (D) and T in Ohmic plasmas were compared. Two rotation reversals per isotope type are observed in plasma density scans spanning the linear and the saturated Ohmic confinement regimes. A clear isotope mass dependence is observed at the higher densities. The magnitude of the core rotation was found to depend on isotope mass, with

[a] See Mailloux *et al* 2022 (https://doi.org/10.1088/1741-4326/ac47b4) for the JET Contributors.
[*] Author to whom any correspondence should be addressed.

stronger co-current rotation observed in H. Change on intrinsic rotation characteristics coexist with a stronger thermal energy confinement in T.

Keywords: intrinsic rotation, isotope mass, tritium plasmas, Ohmic confinement

(Some figures may appear in colour only in the online journal)

1. Introduction

The onset of a spontaneous rotation in magnetically confined plasmas is a physics phenomenon that still lacks a full explanation. In tokamak devices, the so-called intrinsic rotation, is detected in the absence of externally applied momentum [1] and has become a key area of research, as it is expected to play an important role in the performance of future tokamak devices, such as the next step in fusion research, ITER [2], in which momentum input will be small. Some of the beneficial effects of plasma rotation are linked to the increased rotation shear in the plasma core, which leads to both macroscopic magneto-hydro-dynamic (MHD) and turbulence instabilities reduction or even suppression and thus increasing thermal confinement and fusion energy generation. Therefore, determining the intrinsic rotation in future tokamak devices is an essential step. Whereas several studies about the dependences of intrinsic rotation on plasma parameters have been published [3–8], more studies are necessary to clarify two critical aspects. How intrinsic rotation depends on the tokamak size, as ITER will be much larger than present day tokamaks, and how it depends on different hydrogen (H) isotopes, as unlike in most of the present-day experiments, deuterium (D)–tritium (T) mixed plasmas will be used to generate fusion energy.

In order to address such key physics aspects, recent experiments at the Joint European Torus (JET) [9] have been carried out. JET is the largest tokamak in operation and the main link between smaller machines, where intrinsic rotation has been mostly studied, and ITER. Among important JET features for reliable ITER predictions are the ITER-like wall (a Beryllium first wall and a Tungsten divertor [10]), and currently the unique capability to operate with T. For the first time, intrinsic rotation experiments have been performed by including all the different H isotopes, i.e. H, D and T in Ohmic plasmas. One of the objects of the experiments was to study rotation reversals, a puzzling phenomenon commonly observed in small and medium size tokamaks [11], where a transition from monotonic to non- monotonic rotation profiles is observed at a critical density, in some cases leading to plasmas with central and outer regions flowing in opposite directions. The link between intrinsic rotation and thermal confinement has been studied in these sets of experiments that are also the first study of the isotope effect including T plasmas, on the transition from the linear Ohmic confinement (LOC) to the saturated Ohmic confinement (SOC) regime [12].

2. Experimental setup

Density scans in Ohmic plasmas were performed in low triangularity, divertor, configurations with a toroidal magnetic field $B_T = 2.7$ T and plasma current $I_p = 2.3$ MA. The density was varied in steps and toroidal rotation measured during steady state density plateaus (figure 1). The electron density range, with averaged line average values 0.8–3.0 $\times$ $10^{19}\mathrm{m}^{-3}$, was extended with respect to previous JET intrinsic rotation experiments [6, 13]. The operation at densities lower than routinely used at JET, was guided by extrapolation of Alcator C-Mod [14] observations, under the hypothesis that reversals from co- to counter-current rotation at low-densities occur at a fixed value of $N_e q_{95}$ as suggested by Alcator C-Mod observations [15] (where N_e is the electron density and q_{95} the safety factor at the 95% flux surface).

Conditions were matched in H, D and T plasmas, with $Z_{\mathrm{eff}} \sim 1$, for the study of isotope effects. The ion temperature and the toroidal rotation of the main-ion were measured from Hα, Dα or Tα charge exchange spectrum [16, 17] obtained during short bursts of neutral beam injection (NBI). These were the first measurements of the main ion intrinsic rotation from JET plasmas. (Unlike previously reported JET intrinsic rotation that was measured from charge exchange recombination spectroscopy of carbon VI [13], no impurity has been injected or used for diagnostic purposes in these plasmas.) In the following, the rotation data that will be shown are from measurements at the beginning of the NBI power, with a time resolution of 10 ms, when momentum input from NBI is negligible. In the convention used here, positive sign means rotation in the direction of the plasma current. Rotation reversals are defined as a change in sign of the rotation shear in the plasma core. The plasma edge rotates in all cases in co-current direction, as previously observed in JET Ohmic plasmas with no ripple enhancement [13].

3. Experimental results

Previous Ohmic rotation (measured for carbon VI ion) in JET D plasmas had shown hollow profiles [6, 13]. With the extended density range, both peaked and hollow rotation profiles have now been observed (figure 2). For all three H isotopes, as the density increased, two consecutive core rotation reversals were observed. At the lowest density the whole plasma rotates in the co-current direction. By increasing the density, co-current rotation decreased with a reversal

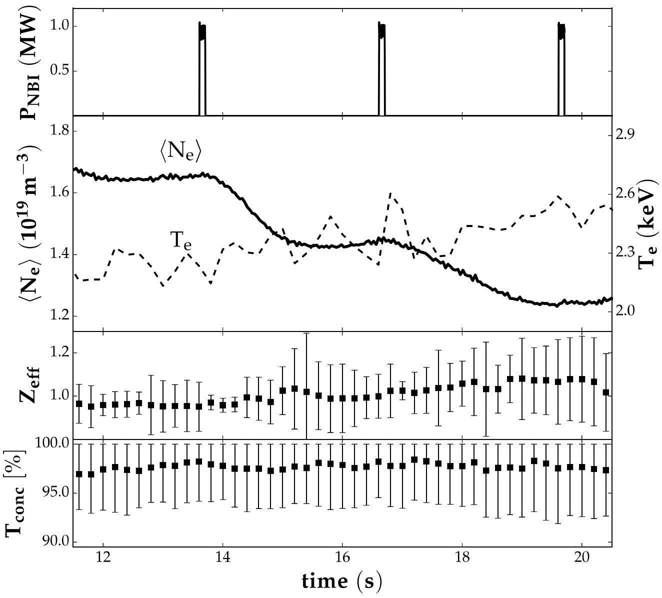

Figure 1. Experimental set up. Tritium plasma #99263 with $I_p = 2.3$ MA and $B_T = 2.7$ T, $q_{95} = 3.5$ (i) P_{NBI} is the NBI power, showing short pulses (blips) for charge exchange measurements at the end of density plateaus; (ii) $<N_e>$ is the line-averaged electron density from far-infrared interferometer, and T_e is the central electron temperature measured with high resolution Thomson scattering (iii) effective charge, Z_{eff}, from visible Bremsstrahlung, (iv) $T_{conc} = N_T/(N_H + N_D + N_T)$ is the tritium concentration.

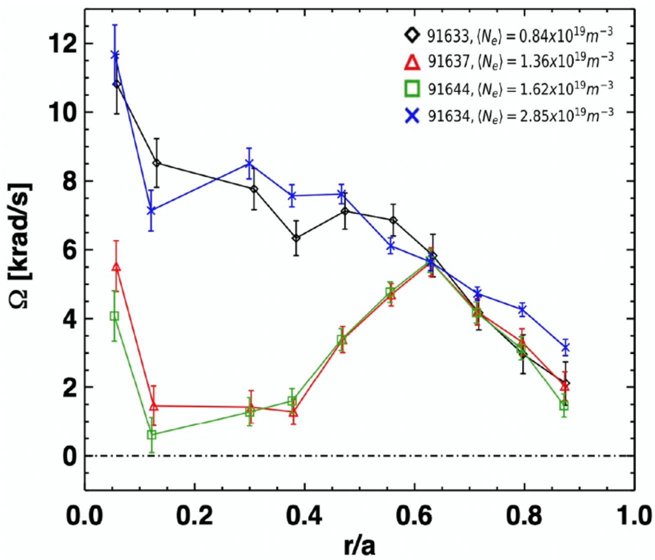

Figure 2. Examples of toroidal angular frequency profiles measured in hydrogen plasmas with $I_p = 2.3$ MA, $B_T = 2.7$ T, as the $<N_e>$, the line-averaged electron density measured with the far-infrared interferometer, increased from 0.84×10^{19} m^{-3}–2.85×10^{19} m^{-3}.

from peaked to hollow profiles. Further increasing the density leads to restoration of monotonic profiles, co-rotation now increasing as a function of density (figures 3(*a*) and (*b*)). For H, the rotation profiles go from peaked to hollow to peaked however the rotation is always co-current (figure 2). Core counter-current rotation was only observed with D and T. In all cases,

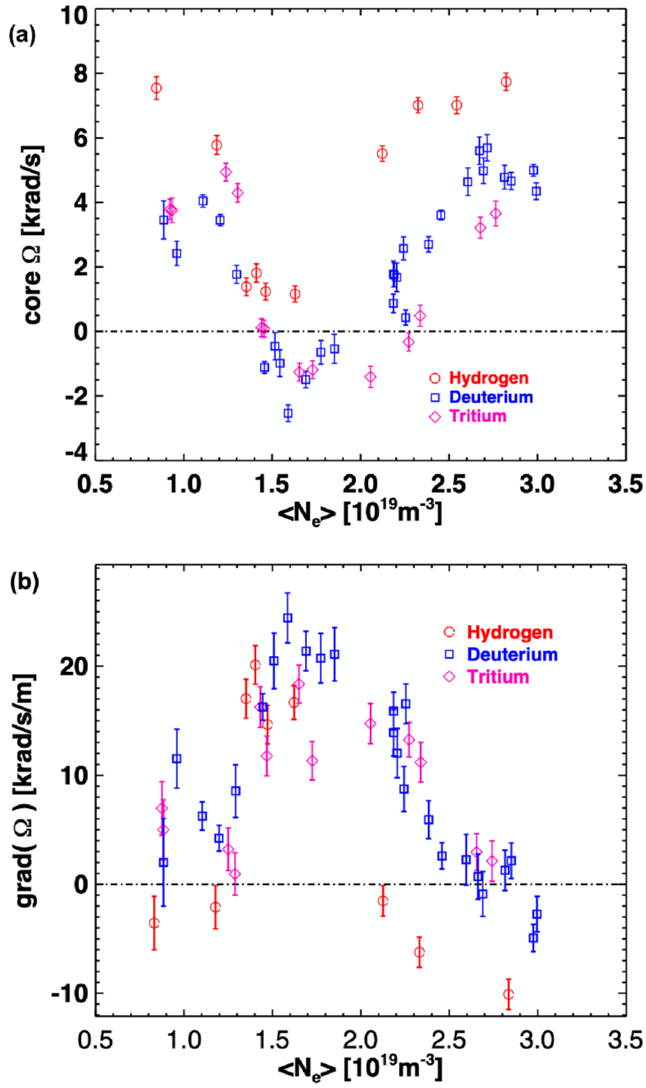

Figure 3. (*a*) Central main ion toroidal rotation angular frequency (average over $r/a = 0.0$–0.3) versus average line density for $I_p = 2.3$ MA, $B_T = 2.7$ T. Hollow profiles have $\Omega < 2$krad s^{-1}. (*b*) Gradient of angular frequency (averaged at $r/a = 0.3$–0.65) versus average line density for $I_p = 2.3$ MA, $B_T = 2.7$ T.

the rotation reversal occurs at a radius larger than the sawtooth inversion radius and does not appear to be related to MHD instability. This was the first time that rotation reversals were observed in JET Ohmic plasmas.

The reversal of the rotation shear at low densities is similar to observations extensively studied in D plasmas in devices smaller than JET, as TCV [18, 19], Alcator C-Mod [14], ASDEX-U [20, 21] and DIII-D [22]. The second transition at higher densities has also been reported from experiments in TCV [19] and ASDEX-U [21]. An interesting observation in JET, is the recovery of co-rotation profiles with the same rotation shear in the high-density branch, as seen in low densities (figure 2). For a review of rotation bifurcations in medium size tokamaks see [11].

The phenomenology is similar in all three isotopes, however the magnitude of the core rotation was found to depend

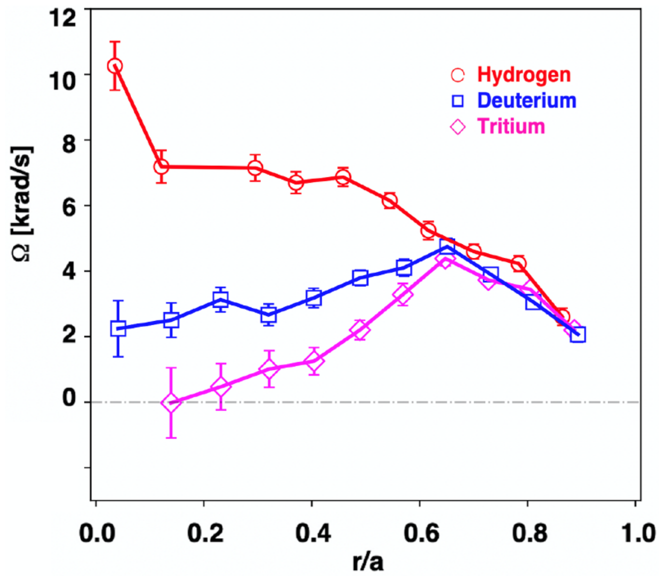

Figure 4. H, D and T toroidal angular frequency profiles with the same density $<N_e> \sim 2.35 \times 10^{19}$ m^{-3}, for plasmas with $I_p = 2.3$ MA, $B_T = 2.7$ T, (pulses = #91634 at 56.41; #94864 at 56.72 s; #100112 at 56.61 s).

on isotope mass, stronger co-current rotation and larger co-current rotation gradients observed in H (figure 3). Deeper counter-current rotation, with the core and edge rotating in opposite directions was observed in D and T, but not in H. Comparison of rotation profiles with the same density for different isotopes, shows that the rotation difference is at the plasma core and not an effect at the edge (figure 4). Figure 3(*a*) shows that within the experimental uncertainty, the critical density for rotation reversal at low density does not depend on isotope mass. However, the critical density for the second reversal does depend on isotope mass, as it shifts to a higher density when the ion mass increases. Access to the high-density branch of co-current rotation occurs at a higher density for T.

The changes in rotation profiles as a function of the density occurred together with changes in thermal energy confinement spanning from the LOC to the SOC regime. Increasing isotope mass increased the thermal energy confinement time, while the LOC–SOC transition shifted to a slightly higher density [23]. As in other machines the first rotation reversal at low densities is observed near the LOC–SOC transition and close to the density of transition from trapped electron mode (TEM) to dominant ion temperature gradient (ITG) mode [11, 22]. Also in the JET experiments, the low-density reversal, for each isotope, does occur close to those two events although simultaneity with either cannot be confirmed. Within the experimental error the low-density rotation reversal occurs at the same density for the three isotopes. This coincides with the LOC–SOC transition density for H, but not for D and T (figure 5) where the LOC–SOC transition is observed when the rotation profiles are already hollow with the core rotating counter-current. This is similar to a recent study in TCV in H, D and He plasmas where the LOC–SOC transition was also found to depend on isotope ion mass [24]. As shown in figure 5, the rotation reversals do not seem to be linked to a particular change of

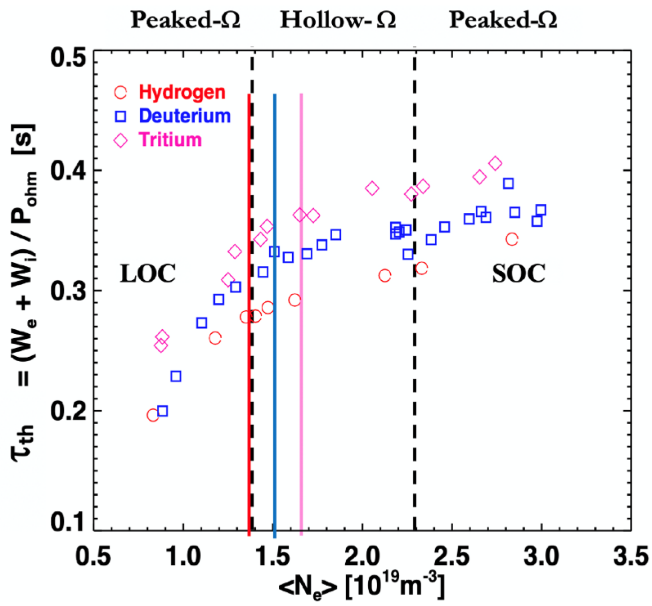

Figure 5. Thermal energy confinement time, τ_{th}, versus average line density for $I_p = 2.3$ MA, $B_T = 2.7$ T. Core counter-rotation was observed within the density values 1.40–2.30 $\times 10^{19}$ m^{-3}, indicated by vertical dashed lines. The LOC–SOC transition for each isotope mass is indicated by solid vertical lines.

the energy content of the plasma with the isotope, as it is always higher with higher isotope mass regardless the rotation profile.

At the density of the LOC–SOC transition a sudden decrease in the magnitude of the normalized gradient of the plasma density was observed, with an associated change in the character of the turbulence. Turbulence linear stability calculations were performed with the gyro-fluid code TGLF [25] and the gyrokinetic code GS2 [26]. The frequency of the

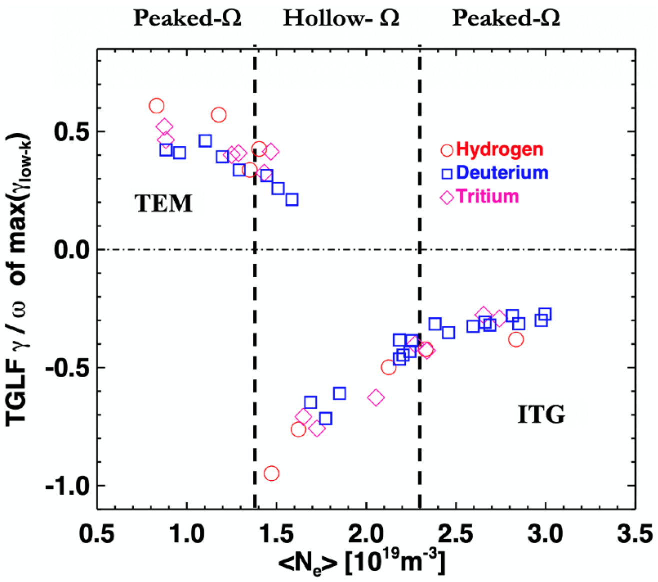

Figure 6. Linear growth rate, γ, divided by ω, the frequency of turbulence dominant mode, for $k\ \rho_s < 0.8$ for radius $r/a = 0.6$ (inside of radius where reversals are observed) from a calculation with TGLF for plasmas with $I_p = 2.3$ MA and $B_T = 2.7$ T. k is the binormal wave number and ρ_s is the ion Larmor radius. Positive values indicate electron-diamagnetic direction. Core counter-rotation was observed within the density values indicated by vertical dashed lines.

turbulence dominant mode for H and D (figure 6) indicates that the TEM–ITG transition occurs at a higher density for D. However, the low-density rotation reversal is at the same density for both isotopes. No particularly obvious abrupt feature of the plasma parameters is observed associated to the rotation second reversal at a higher density. Clearly the type of instability cannot be associated to different directions of core rotation. Co-rotation for all three isotopes, is observed with dominant TEM for the low-densities and ITG for high-densities.

4. Discussion and conclusions

In summary, isotope mass effects on intrinsic rotation were investigated by comparing the main ion rotation observed in H, D, and T Ohmic divertor plasmas in the JET tokamak. Density scans were performed for each isotope, with measurements of main ion intrinsic rotation being obtained in the linear and the saturated Ohmic thermal confinement regimes. The density scans provided the first clear observation of rotation reversals in a large tokamak. As in smaller tokamaks, density has a large effect on the core plasma rotation, producing for each isotope, two plasma rotation reversals in the plasma core. Confirming observations in other devices, the first rotation reversal at low densities occurs close to, though not coinciding with, the LOC–SOC transition and the change from dominant TEM to ITG turbulence. Whilst the critical density for the low-density reversal, within the experimental uncertainty, does not depend on isotope mass, the critical density for the second rotation reversal, increases with ion mass. Comparison of H, D and T rotation profiles, at fixed density, exhibit a clear isotope dependence, with counter-current rotation increasing with ion mass. Access to the high-density branch of co-current rotation requires a higher density for T.

The differences in rotation profiles for different ion masses are only observed in the plasma core. In fact, both the isotope mass and the density effects on the core-rotation profiles occur inside of the same radius, $r/a \sim 0.6$, suggesting that the same physics might explain both phenomena. Most theories for intrinsic rotation attribute the observed rotation to a turbulent redistribution of momentum within the plasma core. Several effects have been invoked to explain this turbulent redistribution [27–33]. For a preliminary analysis of the data, we focus on one of the drives, namely the effect of neoclassical parallel velocity and heat flow on the turbulence [27]. GS2 simulations of this effect have previously shown that as ion–ion collisionality increases, the momentum flux reverses direction in qualitative agreement with the low-density rotation reversal observed in many tokamaks [34]. Using a version of GS2 that includes neoclassical flows, non-linear modeling of rotation profiles covering the whole density range has been performed for the H plasmas [35] and it will be discussed elsewhere. The GS2 simulations reproduce both the low-density and the high-density reversals, and in both cases the change in rotation shear seems to be driven by the change in the shape of the density and temperature profiles, not the change in ion–ion collision frequency. The model and the experimental data agree in the sign of the velocity gradient, with the model predicting velocity gradients smaller than those in experiment. Similar under-predictions have been reported for MAST [36] and ASDEX-U [37]. All the theoretical models of intrinsic rotation based on turbulent momentum redistribution that we are aware of are independent of the ion mass if electrons are assumed to respond adiabatically to the turbulent fluctuations. For this reason, these models cannot explain the observed isotope effect unless the density and temperature profiles are different for different isotopes or the electron response to the turbulent fluctuations depends on the isotope mass, as suggested in [38]. In fact, in these Ohmic plasmas there are several effects that come from ion mass, that can modify the plasma profiles, in particular the electron-ion thermal coupling that is inversely proportional to the mass. Future modeling should include global gyrokinetic simulations that have shown good agreement with core rotation profiles from ASDEX-U [39] and DIII-D [22].

Changes in the rotation with density and with isotope, occur together with changes in thermal confinement. Increasing ion mass leads to higher energy confinement in T and a shift in the density of the LOC–SOC transition with ion mass. Unlike L-mode plasmas with NBI where a positive ion mass effect is observed at the plasma edge and no isotopic effect in the core could be resolved [40], in the Ohmic plasmas both heat confinement and as shown here, the rotation, show isotope mass effects in the plasma core. Detailed analysis of the isotope effect on energy confinement of Ohmic plasmas will be discussed in a separate paper. These JET results are a key input for improved prediction of intrinsic rotation and momentum transport in ITER D–T plasmas.

Acknowledgments

This work has been carried out within the framework of the EUROfusion Consortium, funded by the European Union via the Euratom Research and Training Programme (Grant Agreement No.101052200—EUROfusion). Views and opinions expressed are however those of the authors only and do not necessarily reflect those of the European Union or the European Commission. Neither the European Union nor the European Commission can be held responsible for them. In addition, this work has received financial support from 'Fundação para a Ciência e Tecnologia' through contracts UID/FIS/50010/2013, IF/00483/2014/ CP1214/CT0008 and grant PD/BD/105877/2014.

ORCID iDs

M.F.F. Nave https://orcid.org/0000-0003-2078-6584
J. Ferreira https://orcid.org/0000-0001-5015-7207
J. Garcia https://orcid.org/0000-0003-0900-5564
P.R. Fernandez https://orcid.org/0000-0002-7361-1131
M. Barnes https://orcid.org/0000-0002-0177-1689
F. Casson https://orcid.org/0000-0001-5371-5876
A. Hubber https://orcid.org/0000-0002-3558-8129
A. Kappatou https://orcid.org/0000-0003-3341-1909
C.F. Maggi https://orcid.org/0000-0001-7208-2613

References

[1] Eriksson L.-G., Righi E. and Zastrow K.-D. 1997 *Plasma Phys. Control. Fusion* **39** 27
[2] Ikeda K. 2007 *Nucl. Fusion* **47** E01
[3] Rice J.E., Ince-Cushman A.C., Reinke M.L., Podpaly Y., Greenwald M.J., LaBombard B. and Marmar E.S. 2008 *Plasma Phys. Control. Fusion* **50** 124042
[4] Scarabosio A., Bortolon A., Duval B.P., Karpushov A. and Pochelon A. 2006 *Plasma Phys. Control. Fusion* **48** 663
[5] deGrassie J.S., Rice J.E., Burrell K.H., Groebner R.J. and Solomon W.M. 2007 *Phys. Plasmas* **14** 056115
[6] Eriksson L.-G., Hellsten T., Nave M.F.F., Brzozowski J., Holmström K., Johnson T., Ongena J. and Zastrow K.-D. (JET-EFDA Contributors) 2009 *Plasma Phys. Control. Fusion* **51** 044008
[7] McDermott R.M., Angioni C., Dux R., Gude A., Pütterich T., Ryter F. and Tardini G. (the ASDEX Upgrade Team) 2011 *Plasma Phys. Control. Fusion* **53** 035007
[8] Shi Y. *et al* 2011 *Phys. Rev. Lett.* **106** 235001
[9] Huguet M., Dietz K., Hemmerich J.L. and Last J.R. 1987 *Fusion Technol.* **11** 43
[10] Matthews G.F. *et al* (EFDA-JET contributors) 2011 *Phys. Scr.* **T145** 014001
[11] Camenen Y. *et al* 2017 *Plasma Phys. Control. Fusion* **59** 034001
[12] Parker R., Greenwald M., Luckhardt S., Marmar E., Porkolab M. and Wolfe S. 1985 *Nucl. Fusion* **25** 1127
[13] Nave M.F.F., Johnson T., Eriksson L.-G., Crombé K., Giroud C., Mayoral M.-L., Ongena J., Salmi A., Tala T. and Tsalas M. 2010 *Phys. Rev. Lett.* **105** 105005
[14] Rice J.E. *et al* 2011 *Nucl. Fusion* **51** 083005
[15] Rice J.E. *et al* 2013 *Nucl. Fusion* **53** 093015
[16] Delabie E., Brix M., Giroud C., Jaspers R.J.E., Marchuk O., O'Mullane M.G., Ralchenko Y., Surrey E., von Hellermann M.G. and Zastrow K.D. (JET-EFDA Contributors) 2010 *Plasma Phys. Control. Fusion* **52** 125008
[17] Hawkes N.C., Delabie E., Menmuir S., Giroud C., Meigs A.G., Conway N.J., Biewer T.M., Hillis D.L. and Contributors J.E.T. 2018 *Rev. Sci. Instrum.* **89** 10D113
[18] Bortolon A., Duval B.P., Pochelon A. and Scarabosio A. 2006 *Phys. Rev. Lett.* **97** 235003
[19] Duval B.P., Bortolon A., Karpushov A., Pitts R.A., Pochelon A. and Scarabosio A. (the TCV Team) 2007 *Plasma Phys. Control. Fusion* **49** B195
[20] Angioni C. *et al* (ASDEX Upgrade Team) 2011 *Phys. Rev. Lett.* **107** 215003
[21] McDermott R.M., Angioni C., Conway G.D., Dux R., Fable E., Fischer R., Pütterich T., Ryter F. and Viezzer E. (the ASDEX Upgrade Team) 2014 *Nucl. Fusion* **54** 043009
[22] Grierson B. *et al* 2019 *Phys. Plasmas* **26** 042304
[23] Delabie E., Nave M.M.F., Pablo Rodriguez-Fernandez B., Lennholm L.M. and Biewer T. and (JET Contributors) 2021 *63rd Annual Meeting of the APS Division of Plasma Physics* (*Pittsburgh, PA, 8–12 November 2021*)
[24] Bagnato F. 2022 *28th ITPA-TC 29th March 29th—1st April 2022*
[25] Staebler G.M., Kinsey J.E. and Waltz R.E. 2007 *Phys. Plasmas* **14** 055909
[26] Kotschenreuther M., Rewoldt G. and Tang W.M. 1995 *Comp. Phys. Commun.* **88** 128
[27] Parra F.I. and Catto P.J. 2010 *Plasma Phys. Control. Fusion* **52** 045004
[28] Camenen Y., Peeters A.G., Angioni C., Casson F.J., Hornsby W.A., Snodin A.P. and Strintzi D. 2009 *Phys. Rev. Lett.* **102** 125001
[29] Waltz R.E., Staebler G.M. and Solomon W.M. 2011 *Phys. Plasmas* **18** 042504
[30] Sung T., Buchholz R., Casson F.J., Fable E., Grosshauser S.R., Hornsby W.A., Migliano P. and Peeters A.G. 2013 *Phys. Plasmas* **20** 042506
[31] Barnes M. and Parra F.I. 2019 *Plasma Phys. Control. Fusion* **61** 025003
[32] Parra F.I. and Barnes M. 2015 *Plasma Phys. Control. Fusion* **57** 045002
[33] Stoltzfus-Dueck T. 2019 *Plasma Phys. Control. Fusion* **61** 124003
[34] Barnes M., Parra F.I., Lee J.P., Belli E.A., Nave M.F.F. and White A.E. 2013 *Phys. Rev. Lett.* **111** 055005
[35] Mauriya A. 2020 Effect of impurities in intrinsic rotation of tokamak plasmas *PhD thesis* Instituto Superior Técnico, University of Lisbon
[36] Hillesheim J.C., Parra F.I., Barnes M., Crocker N.A., Meyer H., Peebles W.A., Scannell R. and Thornton A. (the MAST Team) 2015 *Nucl. Fusion* **55** 032003
[37] Hornsby W.A., Angioni C., Fable E., Manas P., McDermott R., Peeters A.G., Barnes M. and Parra F. (The ASDEX Upgrade Team) 2017 *Nucl. Fusion* **57** 046008
[38] Belli E.A., Candy J. and Waltz R.E. 2020 *Phys. Rev. Lett.* **125** 015001
[39] Hornsby W.A., Angioni C., Lu Z.X., Fable E., Erofeev I., McDermott R., Medvedeva A., Lebschy A. and Peeters A.G. (The ASDEX Upgrade Team) 2018 *Nucl. Fusion* **58** 056008
[40] Maggi C.C. 2018 *Plasma Phys. Control. Fusion* **60** 014045